Altering the Reaction Coordinate of the ATP Sulfurylase−GTPase Reaction†

Ming Yang and Thomas S. Leyh*

Department of Biochemistry, Albert Einstein College of Medicine, 1300 Morris Park Avenue, Bronx, New York 10461

Received August 26, 1996; Revised Manuscript Received December 23, 1996⊗

ABSTRACT: ATP sulfurylase, isolated from *Escherichia coli* K-12, catalyzes and couples two reactions: the hydrolysis of GTP and the synthesis of APS (adenosine 5′-phosphosulfate). Its GTPase activity is regulated in response to ligand binding at the APS-forming active site. In particular, AMP mimics an intermediate-like form of the enzyme that increases the k_{cat} for GTP hydrolysis 180-fold. Using equilibrium and pre-steady-state methods, we have determined the relative Gibbs energies for many of the ground and transition states in the GTPase catalytic cycle, in the presence and absence of AMP. GTP and AMP energetically interact throughout the substrate branch of the reaction coordinate; however, once bond breaking occurs, communication between nucleotides ceases. Stopped-flow experiments, using the fluorescent nucleotides 2′-deoxy-mant-GTP and -GDP, indicate that the binding of AMP fosters a conformation of the enzyme that hinders the addition of 2′-deoxy-mant-GTP into the active site without affecting its escaping tendency. These results explain the effects of AMP on the equilibrium binding of the 2′-deoxy-mant-GTP. The second-order rate constants for the binding of 2′-deoxy-mant-GTP or -GDP, $\sim 1 \times 10^{-6}$ M^{-1} s^{-1}, are 2−3 orders of magnitude less than expected for simple diffusion models, and the binding progress curves appear biphasic. These findings suggest the presence of an intermediate(s) in the binding reactions. The Gibbs energy changes that occur in the reaction coordinate upon binding of AMP clearly show that the catalytic effect of AMP is due primarily to its −3.1 kcal/mol stabilization of the rate-limiting transition state.

Regulating the hydrolytic activity of GTPases is pivotal in controlling cellular communication (Bourne et al., 1991). Cleaving the $\beta-\gamma$ bond of GTP is linked to the structural changes that underlie the protein's allosteric properties (Berchtold et al., 1994; Schweins & Wittinghoffer, 1994; Nassar et al., 1995). Typically, only the GTP−GTPase complex is competent to bind to and activate a specific target-(s) (Bourne et al., 1990). The rate constant governing the conversion of E·GTP to E·GDP sets the half-life of the active form of the GTPase. It determines the interval during which a GTPase can transmit the signal that a specific metabolic event has occurred to the appropriate target(s). The half-life of the E·GTP complex expands and contracts as the GTPase enters the various phases of its communication cycle. This often precise temporal regulation, mediated by allosteric effectors, is used in intricate ways to control the fidelity of the interaction of the target with its counterparts (Hopfield, 1974; Thompson, 1988). In this paper we take an in-depth look at how bond breaking is controlled in the ATP sulfurylase−GTPase.

ATP sulfurylase (ATP:sulfate adenylyltransferase, EC 2.7.7.4), cloned from *Escherichia coli* K-12, is a tetramer of heterodimers (Leyh et al., 1987). One of the subunits of the heterodimer, CysN, shows 48% identity and 71% similarity to the so-called GTPase structural core sequence elements (Leyh et al., 1992). ATP sulfurylase catalyzes the reactions (Leyh & Suo, 1992):

$$ATP + SO_4 \rightleftharpoons APS + PP_i \quad (1)$$

$$GTP + H_2O \rightleftharpoons GDP + P_i + H^+ \quad (2)$$

These reactions are kinetically and energetically linked by the enzyme. At pH = 8.0, the equilibrium constant for reaction 1 changes from 1.1×10^{-8} to 0.059 upon addition of a saturating concentration of GTP (Liu et al., 1994a,b). APS is the metabolic precursor of PAPS (3′-phosphoadenosine 5′-phosphosulfate) which is the sulfuryl group donor in transfer reactions that regulate the activity of a variety of physiologically important molecules including estrogen, selectin, and complement C4 (Hortin et al., 1989; Pasqualini et al., 1992; Hemmerich et al., 1994); for reviews see Leyh (1993) and Niers et al. (1994).

The GTP-activated, APS synthesis mechanism includes the random binding of ATP and GTP, followed by GTP hydrolysis which precedes, or is concomitant with, the formation of an E*AMP intermediate (Liu et al., 1994a,b). Pyrophosphate is then released, followed by the addition of sulfate which reacts with the intermediate to form APS. The GTPase activity of ATP sulfurylase is potently regulated by the APS-forming reactants (Wang et al., 1995). Using substrates, and analogues, one can construct nonreactive complexes at the APS-forming active site to investigate linkage between GTP hydrolysis and ligand binding at that site (Wang et al., 1995). The binding of AMP appears to elicit an intermediate-like form of the enzyme, causing a 180-fold increase in the k_{cat} for GTP hydrolysis.

In this paper we describe how the binding of AMP affects the Gibbs energy−reaction coordinate diagram for the GTP hydrolysis reaction. The nucleotides energetically interact through the reaction coordinate up to and including the bond-breaking step, at which point their interactions virtually

† Supported by National Institutes of Health Grant GM54469.

* Corresponding author. Tel: 718-430-2857. Fax: 718-430-8565. E-mail: leyh@aecom.yu.edu.

⊗ Abstract published in *Advance ACS Abstracts,* March 1, 1997.

S0006-2960(96)02140-X CCC: $14.00

disappear. The majority of the catalytic influence of AMP is accounted for by its stabilization of the rate-determining transition state. The catalytic power of the enzyme is evaluated by comparing the kinetic constants of the enzymatic and solution phase hydrolysis reactions. A comparison of the Gibbs energy−reaction coordinate diagrams at 1.0 M and physiological reactant concentrations demonstrates that the efficiency of the enzyme is far greater at the physiological concentrations.

MATERIALS AND METHODS

Materials. 2′-Deoxyguanine nucleotides (sodium salt), AMP (free acid), Hepes,[1] and $MgCl_2$ were purchased from the Sigma Chemical Co. *N*-Methylisatoic anhydride was obtained from Molecular Probes, Inc. Mono-Q fast-flow anion-exchange resin is a product of Pharmacia Chemical Co. Sigma Plot software was purchased from Jandel Scientific.

2′(3′)-O-(*N*-Methylanthraniloyl)guanosine 5′-[β,γ-imido]-triphosphate (mant-GMPPNP) was generously supplied by Martin R. Webb, located at the National Institute for Medical Research, Mill Hill, London.

ATP Sulfurylase. The enzyme was purified according to a published protocol from an *E. coli* K-12 strain containing an expression vector that causes the production of high levels of the *E. coli* K-12 enzyme (Leyh et al., 1987). The specific activity of the enzyme was 0.48 unit/mg (Leyh et al., 1987).

Stopped-Flow Fluorescence Measurements. Measurements were made using a Photophysics (model SX-17MV) instrument. The samples were equilibrated and the experiments performed at 25 ± 2 °C. Our previous studies have shown that the enzyme is stable toward high-velocity mixing (Wang et al., 1995). The samples were excited with 360 nm light (8 nm entrance slit); light emitted above 405 nm was detected (5 nm exit slit). A typical experiment used a 300 V photomultiplier with variable bias offset. The signal from each scan was acquired without filtering; three to five scans were averaged, and in certain cases, a 1.0 ms filter was applied to the data before fitting. The data were fit to a single-exponential model using the instrument's data analysis software which employs a Marquardt fitting algorithm. The concentrations of ligand and enzyme were chosen such that the reactions remained pseudo-first-order with respect to enzyme concentration throughout the progress curve; typically, less that 5% of the enzyme was bound at the end point of the reaction.

Fluorescence Titrations. The titrations were performed by monitoring the change in fluorescent intensity that occurred upon dilution of a solution containing all of the relevant components, including the titrant, with an identical solution that did not contain the titrant. The titration solutions were equilibrated and the experiments performed at 25 ± 2 °C. Two to five intensity measurements, made at each titrant concentration, were averaged to obtain the intensity at that concentration. The results shown in the fluorescence titration figures in this paper represent the average of at least two independent titrations. The titrations were performed on a Perkin-Elmer LS-5B fluorometer. The mant compounds were excited using 360 nm light (5 nm entrance slit); the emitted light was detected a 450 nm (5 nm exit slit).

Fitting the Titration Data. The titrations were curve fit using the Sigma Plot program. The single-site and competition binding models are described by second- and third-order polynomials, respectively. The appropriate roots of these equations were used to fit the data and obtain the binding constants. The Sigma Plot program uses the Marquardt−Levenberg fitting algorithm.

Synthesis of 2′-Deoxy-mant-GDP and 2′-Deoxy-mant-GTP. The following protocol differs in several, slight ways from already published methods (Hiratsuka, 1983; John et al., 1990). 2′-Deoxy-GDP (0.41 mmol) was added to 0.62 mL of water and dissolved. The pH of the solution was adjusted to 9.6 with 5.0 N NaOH. Crystalline *N*-methylisotoic anhydride (0.123 mmol) was slowly added to the stirred nucleotide solution which was maintained at 38 (±2) °C. The pH was kept at 9.6 by addition of NaOH for 2 h, at which point the reaction was complete. The solution was then diluted 15-fold (v/v) with a solution of 10 mM triethylamine (TEA)/HCO_3^- (pH = 7.6) and applied to a 30 mL bed volume of Mono-Q fast-flow resin. The compound was eluted with a 400 mL, 0.010−0.8 M TEA/HCO_3^- (pH = 7.6) linear gradient. The chromatography was performed at 4 °C. The 2′-deoxy-mant-GDP eluted as a single, symmetric, well-isolated peak at 0.66 M TEA/HCO_3^-. The TEA/HCO_3^- was removed with a rotovap. The compound was suspended and dried by rotary evaporation three times in methanol, followed by three times in water. It was then suspended in water and the pH of the solution adjusted to 7.0 (±0.3) using 1.0 N NaOH. The purity of the product was estimated at >95% by determining the areas of the peaks of a 252 nm chromatographic profile of the product obtained with the Mono-Q TEA/HCO_3^- system. The authenticity of the compound was verified by demonstrating that its UV/vis and excitation/emission spectra matched those in the literature (Hiratsuka, 1983). The yield was 48%.

The protocol and results of the 2′-deoxy-mant-GTP synthesis were virtually the same as those for 2′-deoxy-mant-GDP. The significant differences were that a 0.01−1.5 M TEA/HCO_3^- (pH = 7.6) linear gradient was used in the preparative chromatography, and 2′-deoxy-mant-GTP eluted at 0.83 M TEA/HCO_3^-.

RESULTS AND DISCUSSION

Binding of 2′-Deoxy-mant-GDP and GDP. To use 2′-deoxy-mant-GDP as a reporter for interactions between native nucleotides and ATP sulfurylase, it was necessary to determine its binding affinity and stoichiometry. The results of a fluorescence titration experiment designed to evaluate the affinity of 2′-deoxy-mant-GDP are shown in panel A of Figure 1. The open and filled circles represent the experimentally observed and "best-fit" relative intensities, respectively. The experimental and theoretical data are in excellent agreement. The single-site binding model used to fit the data yielded the following fit-parameter estimates: $K_d = 8.47$ (±0.22); $(I/I_0)_{max} = 1.52$ (±0.04). $(I/I_0)_{max}$ is the ratio of the fluorescent intensity of the enzyme-bound to solution phase nucleotide.

The number of guanine nucleotide binding sites per GTPase subunit of ATP sulfurylase was determined in a titration experiment in which the concentration of 2′-deoxy-

[1] Abbreviations: Hepes, 4-(2-hydroxyethyl)-1-piperazineethanesulfonic acid; U (unit), micromoles of substrate converted to product per minute at V_{max}; eu, entropy units (calories K^{-1} M^{-1}).

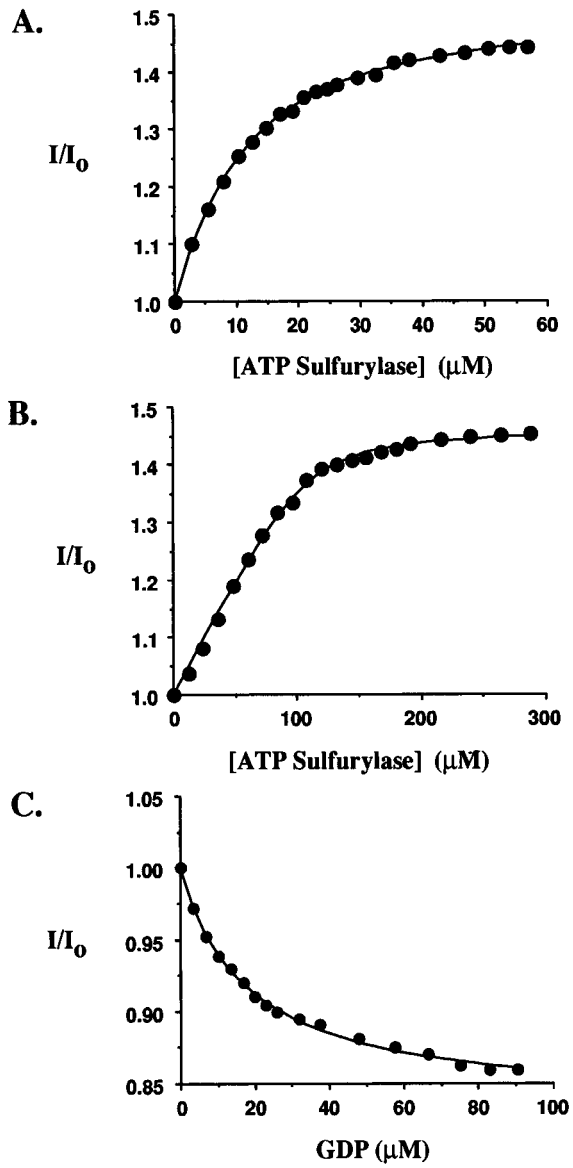

FIGURE 1: Binding interactions of ATP sulfurylase with 2′-deoxy-mant-GDP and GDP. Panel A: Binding affinity of 2′-deoxy-mant-GDP. The strength of the binding interaction was evaluated by fitting the change in nucleotide fluorescence with enzyme concentration using a single-site binding model. The dots represent experimental data; the line through the dots indicates the best fit of the data. The best-fit parameters were $K_d = 8.47$ (± 0.22) μM and $(I/I_0)_{max} = 1.56$ (± 0.035). Panel B: Stoichiometry of binding. The stoichiometry was determined by fitting the change in nucleotide fluorescence with enzyme concentration using a single-site binding model. The dots represent experimental data; the line through the dots indicates the best fit of the data. The best-fit parameters were stoichiometry = 0.9 (± 0.024), $K_d = 6.0$ (± 1.4) μM, and $(I/I_0)_{max} = 1.47$ (± 0.006). Panel C: Binding affinity of GDP. The change in fluorescent intensity of the nucleotide was monitored as 2′-deoxy-mant-GDP was displaced from the active site of ATP sulfurylase by increasing concentrations of GDP. The dots represent experimental data; the line through the dots indicates the best fit of the data. The data were fit using a competitive binding model in which the K_d for GDP and $(I/I_0)_{max}$ were varied to optimize the fit. The best-fit parameters were $K_d = 6.0$ (± 0.23) μM and $(I/I_0)_{max} = 1.47$ (± 0.006). The titration solutions associated with panels A, B, and C contained 2′-deoxy-mant-GDP at 5.0 μM, 120 μM, and 5.0 μM, respectively. The panel C solution contained ATP sulfurylase at 7.5 μM. Each solution contained $MgCl_2$ (1.1 mM) and Hepes (50 mM, pH/K^+ = 8.0). The solutions were equilibriated and the experiments performed at $T = 25$ (± 2) °C.

mant-GDP was held fixed at 14.2 times its K_d (Figure 1, panel B). Under these conditions, one expects a near-linear increase in fluorescent intensity with the enzyme concentration until the ligand and enzyme concentrations are approximately equal, at which point the intensity should plateau quickly. If the data are analyzed by determining the enzyme concentration at which the extrapolated, linear and plateau regions of the isotherm intersect, an estimate of 0.95 nucleotide binding site per GTPase subunit is obtained. Numerically fitting the data yields estimates for this ratio ranging from 0.90 to 0.95, depending on whether K_d and/or $(I/I_0)_{max}$ were allowed to vary during the fitting. These results suggest that the stoichiometry of binding of 2′-deoxy-mant-GDP and ATP sulfurylase is 1:1 and validate using a single-site binding model in analyzing our data.

The affinity of GDP was determined in a competitve binding experiment in which 2′-deoxy-mant-GDP was progressively displaced from ATP sulfurylase by increasing concentrations of the native nucleotide. The results of such an experiment are shown in panel C of Figure 1. The data were numerically fit using the 2′-deoxy-mant-GDP binding parameters discussed above. The dissociation constant for the interaction of GDP and ATP sulfurylase was estimated at $K_d = 6.0$ (± 0.23) μM. This K_d is roughly 10-fold less than that for the interaction of ATP sulfurylase with GTP, which is similar to what is observed for ras/nucleotide interactions (Neal et al., 1988).

ATP sulfurylase couples the hydrolysis of GTP to the formation of a high energy, E*AMP, intermediate which then reacts with sulfate to form activated sulfate or APS. The enzyme is designed to link GTP hydrolysis and the formation of the intermediate. Thus, it is perhaps not surprising that AMP is an excellent activator of GTP hydrolysis (Wang et al., 1995). Allosteric interactions are observed between GTP and AMP throughout the reaction coordinate up to and including the hydrolytic step (Wang et al., 1995); however, what follows hydrolysis has not yet been characterized. To assess the interactions that occur in the product side of the coordinate, the affinity of GDP was studied as a function of AMP concentration.

To investigate the interactions between 2′-deoxy-mant-GDP and AMP, the fluorescence of a solution containing ATP sulfurylase and 2′-deoxy-mant-GDP, each at 5.0 μM, was monitored as the concentration of AMP was increased to a maximum of 9.0 mM. This sensitive experiment can detect changes in quantum yield and/or K_d (provided they are not perfectly compensatory) of as little as ~2%. The open triangles, seen in Figure 2, represent the percent deviation of an individual measurement from the average of all of the measurements. The deviations are quite small (i.e., <1%) and appear randomly scattered about zero. Thus, the interactions between AMP and 2′-deoxy-mant-GDP, if any, are extremely small. This experiment serves as the control for studying the interactions of GDP with AMP. Toward this end, an analogous experiment was performed which was identical to that already described, except that GDP was also present at 5.0 μM. If AMP influenced the affinity of GDP, the intensity of the solution would change due to the linked binding of 2′-deoxy-mant-GDP and GDP. The results (filled dots, Figure 2) are similiar to what is observed in the absence of GDP; that is, the interaction between GDP and AMP is at, or near, zero. It appears that once the effector, AMP, has accomplished the task of facilitating the hydrolysis of

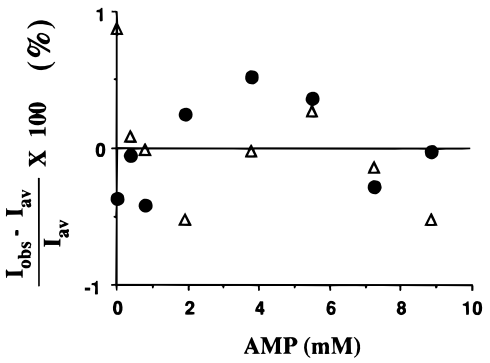

FIGURE 2: Interaction of AMP with 2′-deoxy-mant-GDP and GDP. The changes in fluorescent intensity of solutions containing 2′-deoxy-mant-GDP and ATP sulfurylase, with (△) and without (●) GDP, were monitored as a function of AMP concentration. The nucleotide and enzyme concentrations were near their respective K_d^s. The composition of the titration solutions was as follows: 2′-deoxy-mant-GDP (5.0 μM); GDP (0 or 10 μM); $MgCl_2$ (1.1 mM); Hepes (50 mM, pH/K^+ = 8.0); ATP sulfurylase (7.5 μM). The solutions were equilibrated and the experiments performed at T = 25 (±2) °C. The lack of a significant change in intensity indicates that the guanine and adenine nucleotide interactions are negligible.

GTP, the interaction energy goes essentially to zero. These results further reveal that the γ-phosphoryl moiety is critical to establishing the network of interactions that allow chemical communication between these two nucleotide-binding sites.

Our interpretation of a zero interaction energy for GDP and AMP requires that GDP and AMP bind randomly to the enzyme. Alternatively, AMP might simply not bind to the E·GDP complex. If the latter were true, AMP must also not bind E, since this would result in competition between 2′-deoxy-mant-GDP and AMP for the enzyme, causing a decrease in emitted intensity with increasing AMP concentration. Our previous isotope trapping studies have demonstrated that ATP and GTP bind randomly to ATP sulfurylase (Liu et al., 1994a,b), and our initial rate studies of the AMP-activated hydrolysis of GTP have shown that, even though the binding steps are at equilibrium during turnover (Wang et al., 1995), plots of $1/v$ *versus* 1/[AMP] at fixed variable concentrations of GTP do not intersect on the $1/v$ axis, as is predicted for an ordered scheme with AMP adding last (data not shown). Further support for the random binding of adenine and guanine nucleotides is provided in the following section.

Titrations of mant-GMPPNP with ATP sulfurylase show that the affinity of mant-GMPPNP is, in fact, decreased slightly, from 11.9 (±0.5) μM to 7.5 (±0.2) μM, by the addition of a near-saturating concentration of AMP (panel A, Figure 3). To confirm this effect, a more sensitive experiment was performed in which the fluorescent intensity of a solution containing a fixed concentration of mant-GMPPNP and ATP sulfurylase (each at 5.0 μM) was monitored, as a function of AMP concentration (panel B, Figure 3). The results from panel A predict that the addition of AMP will cause dissociation of the E·mant-GMPPNP complex and a decrease in the emitted intensity—which is what is observed. The experimental result (filled circle) was reasonably well simulated (solid line) using the values for K_d and $(I/I_0)_{max}$ obtained from the data in panel A and previous work (Wang et al., 1995). In an equilibrium-ordered binding scheme the addition of the second ligand can only increase the affinity of the first. As the concentration of the second ligand approaches infinity, so does the

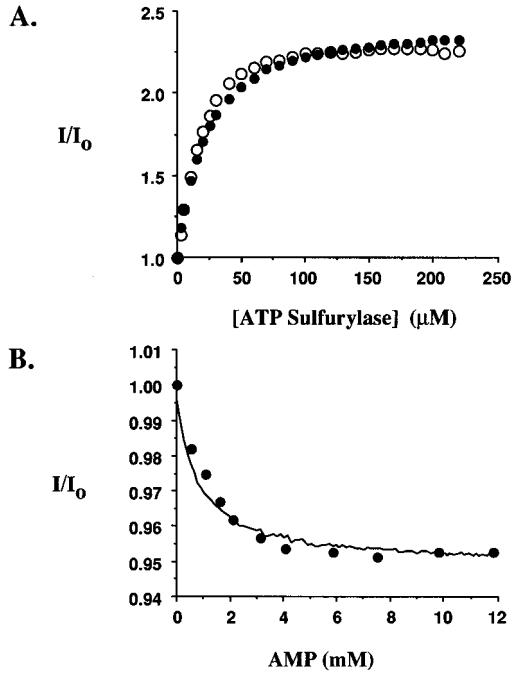

FIGURE 3: Influence of AMP on the binding affinity of mant-GMPPNP. Panel A: The fluorescent intensity of the nucleotide was titrated with ATP sulfurylase in the presence (●) and absence (○) of AMP. A single-site binding model yielded estimates for the nucleotide dissociation constant of 12 (±0.5) μM and 7.5 (±0.25) μM with and without AMP, respectively. The composition of the titration solutions was as follows: mant-GMPPNP (15.0 μM); AMP (0 or 7.4 mM); ATP sulfurylase, at the indicated concentrations; $MgCl_2$ (1.2 mM); Hepes (50 mM, pH/KOH = 8.0); T = 25 (±2) °C. Panel B: The addition of AMP causes mant-GMPPNP to dissociate from the enzyme. To confirm the slight effects demonstrated in panel A, the fluorescent intensity of mant-GMPPNP was monitored as a function of AMP concentration at fixed concentrations of the nucleotide and ATP sulfurylase. The experimental data (●) were simulated (line through data points) using the binding constants obtained from panel A and previous data (Wang et al., 1995). The composition of the titration solution was as follows: mant-GMPPNP (15.0 μM); AMP, at the indicated concentrations; ATP sulfurylase (15.0 μM); $MgCl_2$ (1.2 mM); Hepes (50 mM, pH/K^+ = 8.0); T = 25 (±2) °C.

apparent affinity of the first. Clearly, the interactions between mant-GMPPNP and AMP are inconsistent with ordered binding of these nucleotides. The only simple binding scheme that can explain our data is one in which mant-GMPPNP and AMP bind randomly to the enzyme.

The conformation and orientation of 2′-deoxy-mant-GMPPNP bound at the active site pocket of H-ras is virtually identical to that for the native nucleotide (Scheidig et al., 1995). Given the high degree of similarity among the primary sequences of ATP sulfurylase and other GTPases, it seems likely that mant-GMPPNP will also structurally mimic GTP at the active site of ATP sulfurylase. Nevertheless, GTP and mant-GMPPNP show different binding properties. Mant-GMPPNP binds 6.1-fold more tightly than GTP, and perhaps more importantly, AMP has opposite effects on the binding of mGMPPNP and GTP. The affinity of GTP is increased 3.0 times at a theoretically infinite concentration of AMP (Wang et al., 1995), whereas the binding of GMPPNP is decreased 1.6-fold, at a near-saturating concentration of AMP.

Guanine Nucleotide Binding and Release. Pre-steady-state fluorescence studies using 2′-deoxy-mant nucleotides were performed to determine the rate constants governing the

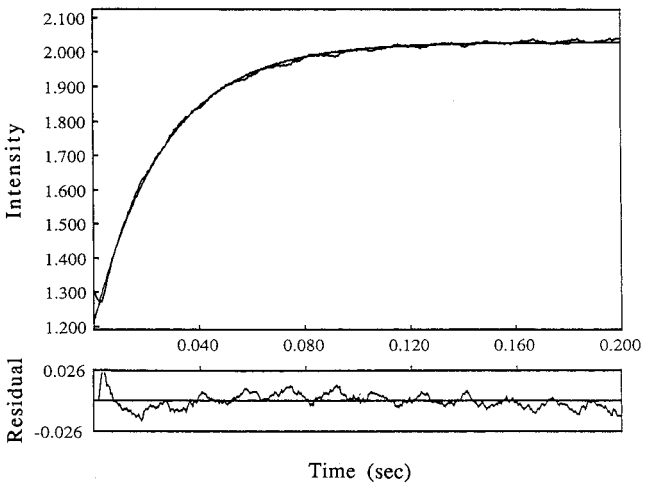

FIGURE 4: Binding of 2′-deoxy-mant-GDP to ATP sulfurylase at saturating AMP. A solution containing ATP sulfurylase (30 μM) was mixed with an equal volume of 2′-deoxy-mant-GTP (0.5 μM); both solutions contained AMP (10 mM), $MgCl_2$ (1.1 mM), and Hepes (50 mM, pH/K^+ = 8.0). The solutions were equilibrated and the experiments performed at 25 (±2) °C. The reaction was monitored by following the change in fluorescent intensity of the nucleotide as it bound to the enzyme. The smooth curve passing through the data represents the best fit to a single-exponential model. The residual plot (the difference between the theoretical and experimental curves) shows slight deviation from single-exponential behavior in the early phase of the reaction.

binding and release of guanine nucleotides to ATP sulfurylase in the presence and absence of AMP. A representative progress curve for a binding reaction at a single enzyme concentration is shown in Figure 4. The minimal model consistent with these data is one in which the binding of ligand occurs in a single, reversible step. However, the residual plot shows slight deviation from single-exponential behavior, indicative of a binding reaction involving more than one step. The binding reactions were studied as a function of enzyme concentration, and the resulting plots of k_{obs} *versus* ATP sulfurylase concentration are shown in Figure 5. Interpreting the data using a single-exponential model yields the on- and off-rate constants tabulated in Table 1. The on-rate constants fall in the range $(1-4) \times 10^6$ M^{-1} s^{-1}, which is 2−3 orders of magnitude less than expected for diffusion-controlled ligand binding to a surface-exposed or buried active site (Alberty & Hammes, 1958; Eigen & Hammes, 1963; Samson & Deutch, 1978). Thus, it appears that these on-rate constants are, in fact, net rate constants and that the binding reactions involve at least two steps, that is, two separate transition state barriers, one of which is the diffusion barrier.

Previous studies using the GTPases, ras (John et al., 1990), and EF-Tu (Wagner et al., 1995) have demonstrated multiple-step binding reactions. In these cases, plots of k_{obs} *versus* guanine nucleotide concentration resemble a rectangular hyperbola, and $k_{on} \sim 0.3-2.1 \times 10^6$ M^{-1} s^{-1}. In both studies, the authors interpret their data using a two-step binding scheme in which enzyme and substrate form a binary complex, which then isomerizes. Their analyses further assume that the first step remains at equilibrium during binding. It should be mentioned that an alternative two-step model (one in which the enzyme must isomerize before the addition of substrate) is equally consistent with their results (Cantor & Schimmel, 1980; Johnson, 1992). Regardless of the precise mechanism, the biphasic dependence of k_{obs} on substrate concentration clearly indicates a minimal, two-step binding reaction. Given these precedents, and the similiar, slow nucleotide on-rate constants, it seems likely that the ATP sulfurylase−GTPase must also pass through a conformational intermediate in its binding reaction to form the reactive, Michealis, complex.

It is interesting that AMP does not measurably influence the off-rate constant for 2′-deoxy-mant-GTP while it decreases the on-rate constant by a factor of 1.3. Thus, it appears that the escaping tendency of the nucleotide from the active site cavity is not affected. The influence on the on-rate constant must mean that the activator is changing the conformation of the enzyme such that the net energetic barrier to the productive docking of the nucleotide is increased.

Energetics of the Catalytic Cycle. The Gibbs potential associated with each of the enzyme species in the GTPase catalytic cycle is plotted *versus* the reaction coordinate in Figure 6. The AMP-activated (dotted lines) and nonactivated (solid lines) profiles are superposed to allow straightforward visualization of the effects of the activator. Panels A and B present the changes in Gibbs energy between enzyme intermediates in the catalytic cycle at 1.0 M and physiological ligand concentrations, respectively. The reference concentrations, or standard states, selected for the Gibbs energy calculations are as follows: uncomplexed Mg^{2+}, 1.0 mM, pH 8.0; all other molecules and complexes (including water and transition states), 1.0 M, ionic strength 0.08−0.11, temperature 25 °C.

As discussed in the *Guanine Nucleotide Binding and Release* section, nucleotide binding is separated into two steps: a diffusion-on step that results in an intermediate (indicated by a prime) and an isomerization that drives the reaction toward product. We have not yet measured the stability of the primed intermediates; hence, the reaction coordinate is interrupted at these points. The activation energy for the addition of nucleotide to the enzyme was calculated assuming a diffusion-limited rate of collision ($k_{on} = 1 \times 10^9$ M^{-1} s^{-1}; $\Delta G^{\circ\ddagger} = 5.2$ kcal/mol). The activation energy for the conversion of the primed to unprimed binary complex was calculated by subtracting the 5.2 kcal/mol diffusion barrier from the $\Delta G^{\circ\ddagger}$ calculated using the rate constants in Table 1.

The Gibbs potentials associated with forming the E·GTP and E·AMP·GTP complexes as well as the activation energies for the rate-determining step were calculated using kinetic and equilibrium constants determined in previous work (Wang et al., 1995). Figure 6 has been drawn such that bond cleavage is rate determining. However, several groups have provided compelling evidence suggesting that the rate-limiting step in the ras-catalyzed hydrolysis of GTP is a conformational step that precedes hydrolysis (Eccleston et al., 1991; Moore et al., 1993). This model is contested by others who, using methods similar to those of the opposing camp, take the position that the hydrolytic step is rate limiting (Rensland et al., 1991). If the former model is correct, the rate-determining barrier in Figure 6 should be subdivided into at least two steps: an isomerization step (with the activation barrier shown) and a non-rate-limiting hydrolytic step.

The region of the reaction coordinate involving the addition of phosphate, outlined in open circles, was estimated using the following considerations. Our studies of the GTP

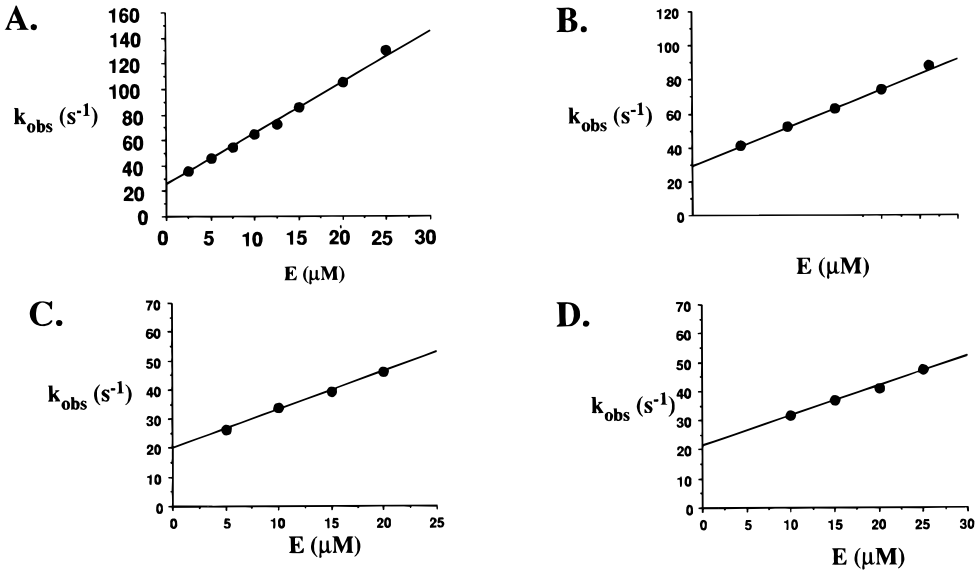

FIGURE 5: Dependence of the rate constant for the addition of nucleotide on enzyme concentration. Panel A: Addition of 2′-deoxy-mant-GDP (0.25 and 0.5 μM) to ATP sulfurylase. Panel B: Addition of 2′-deoxy-mant-GDP (0.25 μM) to ATP sulfurylase at 10 mM AMP. Panel C: Addition of 2′-deoxy-mant-GTP (0.25 μM) to ATP sulfurylase. Panel D: Addition of deoxy-mant-GTP (0.25 μM) to ATP sulfurylase at 10 mM AMP. Solutions containing 2′-deoxy-mant nucleotides (at twice the concentration given above), Hepes (50 mM, pH/K^+ = 8.0), and $MgCl_2$ (1.1 mM) with or without AMP (10.0 mM; i.e., 13.3K_m) were mixed with an equal volume of an identical sample lacking mant nucleotide but containing ATP sulfurylase at a concentration twice that indicated on the *x*-axes of panels A−D. Samples were thermally equilibrated and mixed at 25 (±2 °C).

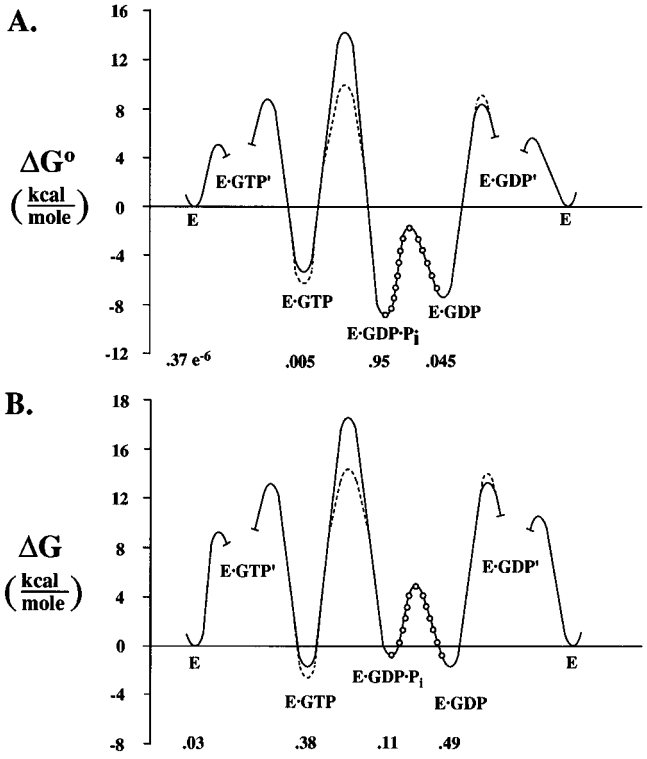

FIGURE 6: Gibbs energy *versus* reaction coordinate diagram. Panel A: The Gibbs energies were calculated at 1.0 M free ligand concentration. Panel B: The Gibbs energies were calculated using physiological free ligand concentrations: GTP (920 μM), GDP (130 μM), and P_i (10 mM). The number beneath a given species indicates the probability that a single molecule of enzyme will reside in that form.

synthesis reaction have determined that the K_m for P_i, at saturating APS and PP_i, is 50 mM (unpublished data). The affinity of P_i for the E·GDP complex of ras is estimated at 12 mM (Neal et al., 1988). In these two cases, the affinity of P_i is in the tens-of-millimolar range. For our ΔG calculations, we have used 50 mM to estimate the affinity of P_i for the E·AMP·GDP and E·GDP complexes. The lower limit for the activation energy associated with the addition of P_i is fixed by the diffusion barrier, 5.2 kcal/mol, which is what is shown. The upper limit is set by the fact that the release barrier must be significantly less (<∼1 kcal/mol) than that for the rate-limiting step.

Table 1: Kinetics of Mant Nucleotide Binding and Dissociation

ligands	k_{off} (s^{-1})[a]	k_{on} (M^{-1} s^{-1})[a]	K_d (μM)[b]
2′-d-mant-GDP	25.9 (±0.8)	3.97 (±0.04) e6	6.5 (±0.25)
2′-d-mant-GDP + AMP	29.5 (±1.68)	4.48 (±0.22) e6	6.6 (±0.50)
2′-d-mant-GTP	20.1 (±0.56)	1.31 (±0.04) e6	15.3 (±0.66)
2′-d-mant-GTP + AMP	21.5 (±0.16)	1.02 (±0.06) e6	21.1 (±1.3)

[a] The values of k_{off} and k_{on} were determined respectively from the slopes and intercepts of the data shown in panels A−D of Figure 5. [b] K_d was calculated using the equation: $K_d = k_{off}/k_{on}$.

Panels A and B present the relative Gibbs energies of the ground and transition states of the enzyme alone. The energetics of the complete system have been "corrected" for the contribution of free ligand to reveal the profile of the enzyme. The strength of this point of view is that it focuses on the behavior of the catalyst, rather than the entire system. This approach, which has been described (Hill, 1976; Pickart & Jencks, 1984), is briefly outlined here: When the binding of the enzyme and ligand is at equilibrium, the molar ratio of the ligand-bound to free enzyme is given by the product of the association constant (K_a) and the ligand concentration [L]. The chemical potential associated with an [EL]/[E] molar ratio at a particular ligand concentration is given by the equation:

$$\Delta G_{EL\text{-}E} = \Delta G^{\circ}_{EL\text{-}E} + RT\ln([EL]/[E]) = \Delta G^{\circ}_{EL\text{-}E} + RT\ln(K_a) + RT\ln[L] \quad (3)$$

$\Delta G_{EL\text{-}E}$ represents the Gibbs energy difference between EL and E at a given ligand concentration and $\Delta G^{\circ}_{EL\text{-}E}$ represents that same difference at 1.0 M concentrations of E, EL, and

L (i.e., the standard state). Equation 3 is applied at each bimolecular step in the reaction coordinate; enzyme isomerizations do not depend on ligand concentration and therefore are not corrected.

The interactions between GTP and AMP occur almost exclusively in the substrate region of the reaction coordinate. The magnitudes of the energetic interactions between the nucleotide-binding sites are small compared to those associated with transitions between ground states and activated complexes; however, they are well positioned to effect catalysis. The primary catalytic effect of AMP is its −3.1 kcal/mol stabilization of the rate-determining transition state. There is a significant, −0.7 kcal/mol, stabilization of the E·GTP ground state which might well be causally linked to the transition-state stabilization. Through selective alterations, AMP fine tunes the reaction coordinate to effect its 180-fold simulation of the enzyme's turnover.

Physiological Ligand Concentration and Enzyme Efficiency. Evolutionary forces, acting over some 2.7 billion years, have fashioned an ATP sulfurylase whose catalytic efficiency has been optimized to satisfy the evolving physiological needs of the organism (Singleton, 1993). Today, in an oxygenated, logarithmically growing *E. coli* cell, ATP sulfurylase finds itself in a *milieu* in which the concentrations of GTP, GDP, and P_i are approximately 920 μM, 130 μM, and 10 mM (Neuhard & Nygaard, 1987; Rao et al., 1993). Using 1.0 M standard states (panel A, Figure 6), one calculates that the probability that an individual enzyme molecule will reside in the product complexes E·GDP or E·GDP·P_i is 99.5%. Such severe product inhibition would likely spell disaster to a cell depending for its survival on the GTPase activity of ATP sulfurylase. The enzyme is a very poor GTPase under these conditions. Of course, it has not evolved to operate at 1.0 M reactant concentrations; the thermodynamic, reactant "push" is very different at physiological conditions.

It is instructive to ask: What is the distribution among the various enzyme species found in the catalytic cycle at physiological ligand concentrations? By applying eq 1, using physiological ligand concentrations, one obtains the Gibbs energy profile of the coordinate shown in panel B of Figure 6. It is immediately apparent that the enzyme is no longer trapped in product forms. Rather, GTP is carried by the enzyme through a series of roughly isoenergetic intermediates to the release of product and regenergation of the reactive enzyme. ATP sulfurylase is well suited to catalyze GTP hydrolysis under physiological conditions.

Catalytic Power of ATP Sulfurylase. One measure of the catalytic power of an enzyme is given by the difference in activation energies of the rate-determining step of the enzyme-catalyzed and solution phase reactions. This difference equals the relative stability of the transition state in the two phases (Wolfenden, 1976; Radzicka & Wolfenden, 1995). The k_{obs} for hydrolysis of MgGTP or MgATP in solution is 2.2×10^{-6}, at 60 °C, which corresponds to a $\Delta G^{\circ\ddagger}$ of 28.2 kcal/mol (Admiraal & Herschlag, 1995). The entropic contribution to the activation energy for the hydrolysis of phosphate monoester dianions is typically quite small, ∼3.7 eu (Di Sabato & Jencks, 1961; Herschlag & Jencks, 1986). Using the entropy of activation for the hydrolysis of the acetyl phosphate dianion, one can estimate that at 25 °C the $\Delta G^{\circ\ddagger}$ for the hydrolysis of GTP is 28.3 kcal/mol. Using k_{cat}/K_m to calculate the activation energy for the enzyme-catalyzed hydrolysis reaction, one obtains values of 10.8 and 14.5 kcal/mol for the AMP-activated and nonactivated reactions, respectively. Thus, the AMP-activated, ATP sulfurylase-catalyzed transition state is 17.5 kcal/mol more stable than that in solution, which gives rise to a 7×10^{12}-fold rate acceleration.

CONCLUSIONS

This paper focuses on several mechanistic aspects of the ATP sulfurylase−GTPase reaction in an attempt to understand the energetic basis of allostery in this system. The equilibrium and microscopic rate constants governing the interactions of guanine nucleotides with the enzyme have been determined in the presence and absence of AMP. These constants have been assembled into an energetic description of the reaction coordinate that clearly demonstrates the mechanism of allostery in this system. AMP and GTP interact throughout the substrate branch of the reaction coordinate, and the nucleotidyl interactions cease once the $\beta-\gamma$ bond of GTP is broken. The AMP-induced rate acceleration occurs primarily through selective stabilization of the transition state. These findings provide an in-depth view of how bond breaking is regulated in the ATP sulfurylase-associated GTPase.

ACKNOWLEDGMENT

We thank Jaing Wei, a postdoctoral fellow in this laboratory, for his valuable assistance in developing the algebraic solution to the competition binding model that was used to fit our data. We also thank Martin R. Webb, at the National Institute for Medical Research, Mill Hill, London, for suppling the mant-GMPPNP used in these studies.

REFERENCES

Admiraal, S. J., & Herschlag, D. (1995) *Chem. Biol. 2*, 729−739.
Alberty, R. A., & Hammes, G. G. (1958) *J. Phys. Chem. 62*, 154−159.
Berchtold, H., Reshetnikova, L., Reiser, C. O., Schirmer, N. K., Sprinzl, M., & Hilgenfeld, R. (1994) *Nature 365*, 126−132.
Bourne, H. R., Sanders, D. A., & McCormick, F. (1990) *Nature 348*, 125−132.
Bourne, H. R., Sanders, D. S., & McCormick, F. (1991) *Nature 349*, 117−126.
Cantor, C. R., & Schimmel, P. R. (1980) *Biophysical Chemistry*, pp 912−913, W. H. Freeman, San Francisco.
Di Sabato, G., & Jencks, W. P. (1961) *J. Am. Chem. Soc. 83*, 4400−4405.
Eccleston, J. F., Moore, K. J., Brownbridge, G. G., Webb, M. R., & Lowe, P. N. (1991) *Biochem. Soc. Trans. 19*, 432−437.
Eigen, M., & Hammes, G. G. (1963) *Adv. Enzymol. 25*, 1−38.
Hemmerich, S., Bertozzi, C. R., Leffler, H., & Rosen, S. D. (1994) *Biochemistry 33*, 4820−4829.
Herschlag, D., & Jencks, W. P. (1986) *J. Am. Chem. Soc. 108*, 7938−7946.
Hill, T. (1976) *Nature 263*, 615−618.
Hiratsuka, T. (1983) *Biochim. Biophys. Acta 742*, 496−508.
Hopfield, J. J. (1974) *Proc. Natl. Acad. Sci. U.S.A. 71*, 4135−4139.
Hortin, G. L., Farries, T. C., Graham, J. P., & Atkinson, J. P. (1989) *Proc. Natl. Acad. Sci. U.S.A. 86*, 1338−1342.
John, J., Sohmen, R., Feuerstein, J., Linke, R., Wittinghofer, A., & Goody, R. S. (1990) *Biochemistry 29*, 6058−6065.
Johnson, K. A. (1992) *Enzymes*, pp 1−61, Academic Press, San Diego.
Leyh, T. S. (1993) *Crit. Rev. Biochem. Mol. Biol. 28*, 515−542.
Leyh, T. S., & Suo, Y. (1992) *J. Biol. Chem. 267*, 542−545.
Leyh, T. S., Taylor, J. T., & Markham, G. H. (1987) *J. Biol. Chem. 263*, 2409−2416.

Leyh, T. S., Vogt, T. F., & Suo, Y. (1992) *J. Biol. Chem. 267*, 10405−10410.
Liu, C., Martin, E., & Leyh, T. S. (1994a) *Biochemistry 33*, 2042−2047.
Liu, C., Suo, Y., & Leyh, T. S. (1994b) *Biochemistry 33*, 7309−7314.
Moore, K. J. M., Webb, M. R., & Eccleston, J. F. (1993) *Biochemistry 32*, 7451−7459.
Nassar, N., Horn, G., Herrmann, C., McCormic, F., & Wittinghofer, A. (1995) *Nature 271*, 554−560.
Neal, S. E., Eccleston, J. F., Hall, A., & Webb, M. R. (1988) *J. Biol. Chem. 263*, 19718−19722.
Neuhard, J., & Nygaard, P. (1987) in *Escherichia coli and Salmonella typhimurium Cellular and Molecular Biology* (Neidhardt, F. C., Ed.) pp 445−473, American Society for Microbiology, Washington, DC.
Niers, C., Beisswanger, R., & Huttner, W. B. (1994) *Chem. Biol. Interact. 92*, 257−271.
Pasqualini, J. K., Schatz, B., Varin, C., & Nguyen, B. L. (1992) *J. Steroid Biochem. Mol. Biol. 41*, 323−329.
Pickart, C. M., & Jencks, W. P. (1984) *J. Biol. Chem. 259*, 1629−1643.
Radzicka, A., & Wolfenden, R. (1995) *Science 267*, 90−93.
Rao, N. N., Roberts, M. F., Torriani, A., & Yashphe, J. (1993) *J. Bacteriol. 175*, 74−79.
Rensland, H., Lautwein, A., Wittinghofer, A., & Goody, R. S. (1991) *Biochemistry 30*, 11181−11185.
Samson, R., & Deutch, J. M. (1978) *J. Chem. Phys. 68*, 285−290.
Scheidig, A. J., Franken, S. M., Carrie, J. E., Reid, G. P., Wittinghofer, A., Pai, E. F., & Goody, R. S. (1995) *J. Mol. Biol. 253*, 132−150.
Singleton, R. J. (1993) in *The Sulfate Reducing Bacteria: Contemporary Perspectives* (Odom, J. M., & Singleton, R. J., Eds.) pp 1−20, Springer-Verlag, New York.
Thompson, R. (1988) *Trends Biochem. Sci. 13*, 91−93.
Wagner, A., Simon, I., Sprinzl, M., & Goody, R. S. (1995) *Biochemistry 34*, 12535−12542.
Wang, R., Liu, C., & Leyh, T. S. (1995) *Biochemistry 34*, 490−495.
Wolfenden, R. (1976) *Annu. Rev. Biophys. Bioeng. 5*, 271−306.

BI962140K